Journal of Biomolecular NMR, 8 (1996) 98–104
ESCOM

J-Bio NMR 374

Phase labeling of C-H and C-C spin-system topologies: Application in PFG-HACANH and PFG-HACA(CO)NH triple-resonance experiments for determining backbone resonance assignments in proteins

Wenqing Feng, Carlos B. Rios and Gaetano T. Montelione*

Department of Molecular Biology and Biochemistry and Center for Advanced Biotechnology and Medicine, Rutgers University, 679 Hoes Lane, Piscataway, NJ 08854-5638, U.S.A.

Received 1 April 1996
Accepted 7 June 1996

Keywords: Automated analysis of NMR data; Glycine; Phase information; Pulsed-field gradient; Spin-system topologies

Summary

Triple-resonance experiments can be designed to provide useful information on spin-system topologies. In this paper we demonstrate optimized proton and carbon versions of PFG-CT-HACANH and PFG-CT-HACA(CO)NH 'straight-through' triple-resonance experiments that allow rapid and almost complete assignments of backbone H^{α}, $^{13}C^{\alpha}$, ^{15}N and H^{N} resonances in small proteins. This work provides a practical guide to using these experiments for determining resonance assignments in proteins, and for identifying both intraresidue and sequential connections involving glycine residues. Two types of delay tunings within these pulse sequences provide phase discrimination of backbone Gly C^{α} and H^{α} resonances: (i) C-H phase discrimination by tuning of the refocusing period τ_{a_f}; (ii) C-C phase discrimination by tuning of the ^{13}C constant-time evolution period $2T_c$. For small proteins, C-C phase tuning provides better S/N ratios in PFG-CT-HACANH experiments while C-H phase tuning provides better S/N ratios in PFG-CT-HACA(CO)NH. These same principles can also be applied to triple-resonance experiments utilizing ^{13}C-^{13}C COSY and TOCSY transfer from peripheral side-chain atoms with detection of backbone amide protons for classification of side-chain spin-system topologies. Such data are valuable in algorithms for automated analysis of resonance assignments in proteins.

Triple-resonance experiments provide an important approach for determining resonance assignments in proteins (Ikura et al., 1990; Montelione and Wagner, 1990; Bax and Grzesiek, 1993). Recent developments have focused on obtaining information useful for classifying amino acid spin-system types (Montelione et al., 1992; Grzesiek and Bax, 1993; Lyons and Montelione, 1993; Wittekind and Mueller, 1993; Yamazaki et al., 1993,1995; Olejniczak and Fesik, 1994; Gehring and Guittet, 1995; Grzesiek and Bax, 1995; Tashiro et al., 1995). This information is extremely valuable for determining resonance assignments, especially when combined with characteristic ^{13}C chemical shift data into automated assignment programs (Friedrichs et al., 1994; Meadows et al., 1994; Zimmerman et al., 1994; Zimmerman and Montelione, 1995). Information about spin-system topologies can be obtained by appropriate tuning of scalar coupling effects. For example, constant-time frequency evolution periods commonly used in triple-resonance experiments for homonuclear ^{13}C-^{13}C decoupling are generally designed to combine frequency evolution and coherence defocusing/refocusing periods (Powers et al., 1991; Clubb et al., 1992; Kay et al., 1992a; Olejniczak et al., 1992; Palmer et al., 1992). During these coherence defocusing/refocusing periods, magnetization oscillates differently according to the spin-system topology and the set of active and passive scalar couplings. In uniformly ^{13}C-enriched molecules, proper tuning of these delay times can provide ^{13}C-resonance phase information (i.e. positive or negative peak intensities) which depends on the number of coupled ^{13}C nuclei (Grzesiek and Bax, 1992b,1993; Santoro and King, 1992; Wittekind and Mueller, 1993; Tashiro et al., 1995).

*To whom correspondence should be addressed.

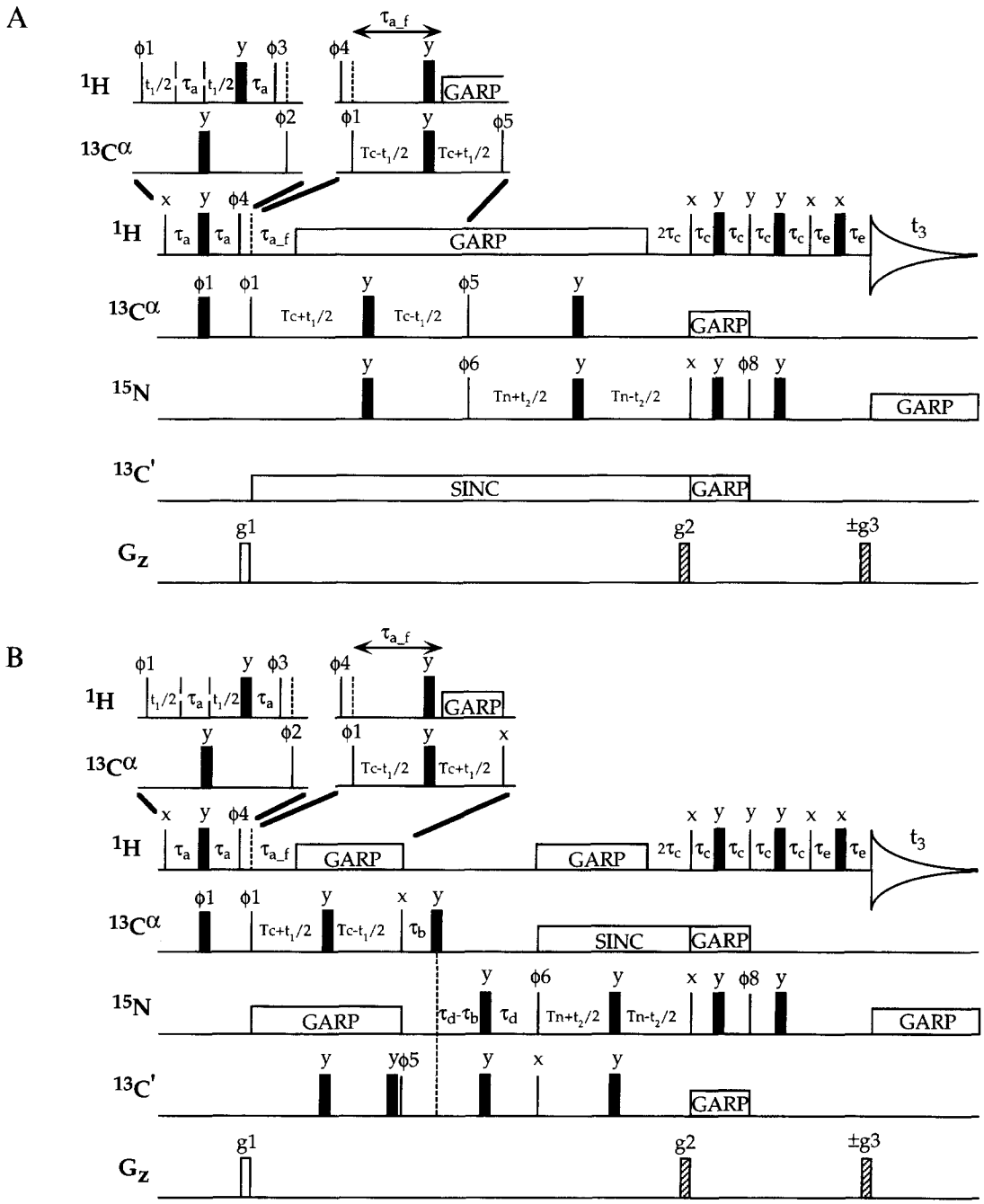

Fig. 1. Pulse sequences for 3D proton ($\omega_1 = {}^1H$) and carbon ($\omega_1 = {}^{13}C$) versions of (a) PFG-CT-HACANH and (b) PFG-CT-HACA(CO)NH experiments. In both pulse sequences, the first inset shows the variant using $\omega_1 = {}^1H$ (rather than $\omega_1 = {}^{13}C$) frequency labeling and the second insert shows the variant implemented by the pulse sequence program for τ_{a_f} values greater than T_c. Coherence transfer delays were tuned to $\tau_a = 1.7$ ms, $\tau_c = 2.8$ ms, $\tau_e = gt3 +$ a gradient recovery time of 110 μs, and $T_n = 14$ ms in both experiments. The HACA(CO)NH experiment used the additional delays $\tau_b = 4.2$ ms and $\tau_d = 13.0$ ms. Pulsed-field gradients were applied along the z-axis with an amplitude of ~26 G/cm. Gradient $g_1 = 100$ μs is a heteronuclear zz-filter (Montelione and Wagner, 1989a) while gradients $g_2 = 5.6$ ms and $g_3 = 500$ μs are used for coherence pathway selection. Wide-band GARP-1 (Shaka et al., 1985) and band-selective SINC decoupling schemes were executed from waveform generators. Dashed vertical lines indicate delimiters of time intervals. Quadrature detection in the t_1 dimension is obtained by changing the phase ϕ_1 in the States-TPPI manner (Marion et al., 1989). The phases are cycled as: $\phi_2 = x,-x$; $\phi_3 = \phi_4 = 4(y),4(-y)$; $\phi_5 = x,x,-x,-x$; $\phi_6 = 8(x),8(-x)$ and receiver phase $= +,-,-,+,-,+,+,-,-,+,+,-,+,-,-,+$. The phase cycle ϕ_6 is optional. For quadrature detection in the t_2 dimension, N- and P-type fid's are collected by inverting the phases of ϕ_8 and g_3 simultaneously, and combined to give pure phase spectra with sensitivity enhancement (Nagayama, 1986; Kay et al., 1992b). The pulse sequences and decoupling waveforms were executed on a three-channel Varian Unity 500 NMR spectrometer equipped with a fourth synthesizer for C' decoupling, and are available by anonymous ftp from nmrlab.cabm.rutgers.edu. or over the world-wide web at http://www-nmr.cabm.rutgers.edu.

We refer to these as 'C-C-type phase experiments'. Alternatively, proper tuning of the time period used for refocusing (or defocusing) antiphase $H_zC_{x,y}$ carbon magnetization into (or from) in-phase carbon magnetization

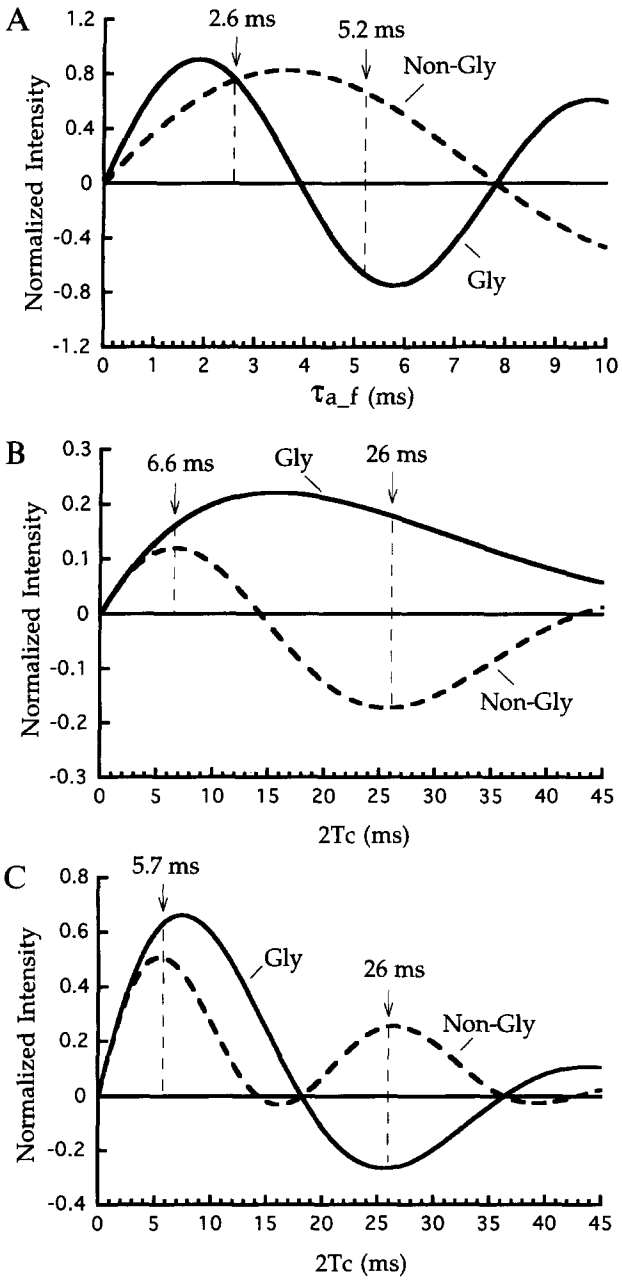

Fig. 2. Dependence of magnetization transfer functions on (a) τ_{a_f} in both PFG-CT-HACANH and PFG-CT-HACA(CO)NH; (b) $2T_c$ in PFG-CT-HACANH; and (c) $2T_c$ in PFG-CT-HACA(CO)NH. Curves are shown for both Gly ($C^{\alpha}H_2$, solid line) and non-Gly ($C^{\alpha}H$, dashed line) spin systems, and correspond to Eqs. 1, 2 and 4, respectively, in the text multiplied by the relaxation term $\exp(-t/T_{2,eff})$. These curves were generated assuming $^1J(C^{\alpha}\text{-}H^{\alpha}) = 128$ Hz, $^1J(C^{\alpha}\text{-}C^{\beta}) = 35$ Hz, $^1J(C^{\alpha}\text{-}C') = 55$ Hz, $^1J(C^{\alpha}\text{-}N) = 11$ Hz, $^2J(C^{\alpha}\text{-}N) = 7$ Hz, and $T_{2,eff} = 20$ ms. Optimal values for τ_{a_f} and $2T_c$ for phase and non-phase spectra are indicated. In this simulation, $T_{2,eff}$ is defined as the effective relaxation time for coherences during the $2T_C$ and τ_{a_f} periods. Although in fact the magnetization passes through different states during these time periods, we make the simplifying (though formally incorrect) assumption that during these refocusing/defocusing periods the coherences of interest relax with a uniform effective relaxation time, $T_{2,eff}$.

can provide ^{13}C-resonance phase information which depends on the number of coupled ^1H nuclei (Morris, 1980; Gehring and Guittet, 1995). We refer to these as 'C-H-type phase experiments'. Such 'phase experiments' can be used to identify spin-system topologies characteristic of different amino acid residue types (see for example Grzesiek and Bax, 1993; Tashiro et al., 1995).

While there are several varieties of side-chain spin-system types, there are only two kinds of C^{α} carbons in a polypeptide chain composed of the 20 common naturally occurring amino acid residues, i.e. methylene Gly C^{α} atoms with no directly coupled C^{β} atoms and methine non-Gly C^{α} atoms with a single directly coupled C^{β} atom. Magnetization pathways involving Gly C^{α} resonances can therefore be distinguished with either C-C-type or C-H-type phase information. Several triple-resonance experiments using ^{13}C-^{13}C COSY (Grzesiek and Bax, 1992a,b, 1993; Wittekind and Mueller, 1993) or TOCSY (Tashiro et al., 1995) transfers to correlate side-chain ^{13}C and/or ^1H resonances with backbone H^N resonances have been described which distinguish Gly C^{α} resonances on the basis of ^{13}C-^{13}C coupling topology. However, these experiments are generally carried out with delays optimized for detecting β or more peripheral resonances, and do not provide as high a sensitivity for detecting backbone ^{13}C and/or ^1H resonances as experiments designed specifically for backbone correlations. In backbone 2D HN(CO)CA (Gehring and Guittet, 1995) and 3D HN(CA)HA-Gly (Wittekind et al., 1993) pulse sequences, selection of Gly C^{α} resonances and suppression of non-Gly C^{α} resonances is obtained on the basis of their different C-H coupling topologies. Unfortunately, these experiments provide only intraresidue Gly or sequential Gly-X peaks, and are generally carried out in addition to experiments tuned for identifying intraresidue and sequential connectivity information for the remaining non-Gly spin systems.

In our efforts to develop automated methods for determining resonance assignments in proteins, we have found that it is convenient to incorporate Gly 'phase labeling' directly into the standard experiments used for establishing intraresidue and/or sequential $C_i^{\alpha}/H_i^{\alpha} \rightarrow NH_i$ or $C_i^{\alpha}/H_i^{\alpha} \rightarrow NH_{i+1}$ connectivities. Using a family of backbone triple-resonance experiments developed in our laboratory over the last few years, we have compared the 'C-C phase' and 'C-H phase' methods for distinguishing Gly from non-Gly spin systems. Pulse schemes for these 3D PFG-CT-HACANH and 3D PFG-CT-HACA(CO)NH experiments are shown in Fig. 1. These pulse sequences have been used in several published structure determinations, but have not previously been described in the literature. They are sensitivity-enhanced, constant-time, PFG versions of the HACANH (Montelione and Wagner, 1989b,1990; Kay et al., 1991; Boucher et al., 1992) and HACA(CO)NH (Boucher et al., 1992) straight-through triple-resonance experiments. These experiments provide data for establishing intraresidue and sequential connections between backbone ^1H, ^{13}C, and ^{15}N atoms with high

sensitivity, while simultaneously yielding selective phase information on glycine spin systems.

In these pulse sequences (Fig. 1) the delay periods τ_{a_f} and $2T_c$ can be adjusted to provide 'C-H' or 'C-C' phase information, respectively. To illustrate this point, we describe transfer functions for $-C^{\alpha}H-C^{\beta}$ and $-C^{\alpha}H_2$ spin systems of the relevant pulse sequence fragments. For all of the experiments outlined in Fig. 1, the transfer function for in-phase carbon magnetization after the refocusing delay τ_{a_f} is multiplied by the following term describing the refocusing of antiphase ^{13}C magnetization by $^1J(C^{\alpha}-H^{\alpha})$ scalar coupling:

$$m[\sin(\pi J_{CH}\tau_{a\_f})\cos^{m-1}(\pi J_{CH}\tau_{a\_f})] \quad (1)$$

where J_{CH} is the $^1J(C^{\alpha}-H^{\alpha})$ coupling constant and m is the number of protons directly bonded to the C^{α} carbon. This 'τ_{a_f} transfer function' is plotted in Fig. 2A. Appropriate tuning of τ_{a_f} can thus be used to discriminate magnetization beginning on Gly (m = 2) and non-Gly (m = 1) C^{α} nuclei based on C-H phase information. Similar considerations can be used to describe the C-C phase effects of $^1J(C^{\alpha}-C^{\beta})$ coupling during the constant-time evolution periods $2T_c$ (Fig. 1). For HACANH and HACA(CO)NH experiments, the transfer function is multiplied by the following terms describing the effects of $^{13}C-^{13}C$ and $^{13}C-^{15}N$ scalar coupling during the period $2T_c$:

$$\sin(2\pi J_{C^{\alpha}N}T_c)\cos(2\pi J_{C^{\alpha}N_{i+1}}T_c)\cos^n(2\pi J_{C^{\alpha}C^{\beta}}T_c) \text{ intra} \quad (2)$$

$$\cos(2\pi J_{C^{\alpha}N}T_c)\sin(2\pi J_{C^{\alpha}N_{i+1}}T_c)\cos^n(2\pi J_{C^{\alpha}C^{\beta}}T_c) \text{ seq} \quad (3)$$

$$\sin(2\pi J_{C^{\alpha}C'}T_c)\cos^n(2\pi J_{C^{\alpha}C^{\beta}}T_c) \quad \text{seq} \quad (4)$$

where $J_{C^{\alpha}N}$, $J_{C^{\alpha}N_{i+1}}$, $J_{C^{\alpha}C^{\beta}}$, and $J_{C^{\alpha}C'}$ are the $^1J(C^{\alpha}-N)$, $^2J(C^{\alpha}-N_{i+1})$, $^1J(C^{\alpha}-C^{\beta})$, and $^1J(C^{\alpha}-C')$ coupling constants, respectively, and n is the number of C^{β} carbon atoms with active one-bond coupling to the C^{α} atom. Equations 2 and 3 describe the intraresidue and sequential $H^{\alpha} \rightarrow H^N$ transfer pathways in HACANH, respectively, while Eq. 4 describes the sequential $H^{\alpha} \rightarrow H^N$ transfer pathway in HACA(CO)NH. These 'T_c transfer functions', Eqs. 2 and 4, are plotted in Figs. 2B and 2C, respectively. Tuning of T_c can thus be used to discriminate magnetization beginning on Gly (n = 0) and non-Gly (n = 1) C^{α} nuclei based on C-C phase information.

In the case of C-H phase tuning (Fig. 2A), the signal modulation is dominated by the $^1J(C^{\alpha}-H^{\alpha})$ coupling constant during τ_{a_f}. Optimal values of τ_{a_f} for maximizing both the methine and the methylene magnetizations are

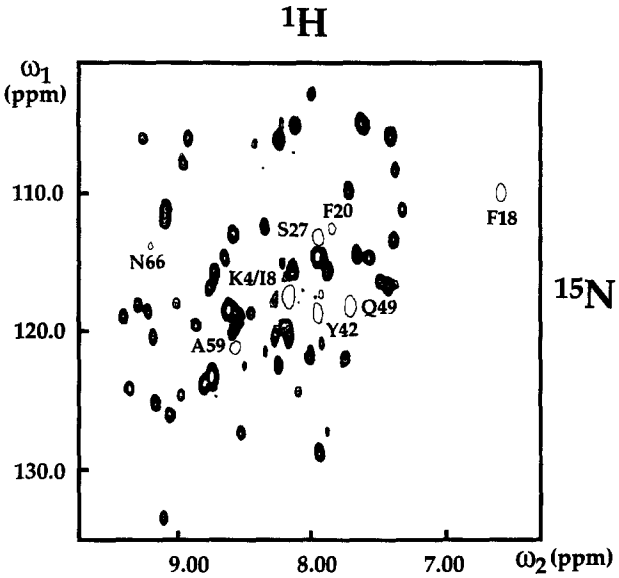

Fig. 3. 2D $^{15}N-H^N$ PFG-CT-HACA(CO)NH spectrum recorded with C-H-type Gly phase information on a uniformly $^{15}N,^{13}C$-enriched sample of the major cold-shock protein A (CspA) from *E. coli*. Peaks with negative phases (i.e. backbone amide N-H correlations of residues which follow Gly residues in the sequence) are drawn with a single contour, while those with positive phases are drawn with multiple contours. The sample at pH 6.0 and temperature of 30 °C had a protein concentration of ~1 mM. Data were recorded at 500 MHz using 64 scans per fid, 100 complex fid's in the ^{15}N dimension, τ_{a_f} = 5.2 ms, $2T_c$ = 5.7 ms, and other instrumental parameters set as described in the legend of Fig. 1. The total collection time was ~2 h.

TABLE 1
COMPARISON OF SIGNAL-TO-NOISE RATIOS IN PFG-CT-HACANH AND PFG-CT-HACA(CO)NH EXPERIMENTS

	τ_{a_f} (ms)	$2T_c$ (ms)	Gly	Non-Gly	Gly-X	Non-Gly-X
HACANH						
Non-phase	2.6	6.6	1.0	1.0		
C-H phase tuning	5.2	6.6	−0.7 ± 0.1 (8)	0.5 ± 0.1 (32)		
C-C phase tuning	2.6	26.0	−0.5 ± 0.2 (8)	1.5 ± 0.4 (32)		
HACA(CO)NH						
Non-phase	2.6	5.7			1.0	1.0
C-H phase tuning	5.2	5.7			−1.2 ± 0.2 (6)	0.7 ± 0.2 (35)
C-C phase tuning	2.6	26.0			−0.2 ± 0.2 (6)	0.5 ± 0.2 (35)

Signal-to-noise ratios were measured for well-resolved peaks in 2D $^{15}N-H^N$ PFG-CT-HACANH and PFG-CT-HACA(CO)NH spectra. The reported values were obtained by dividing the average S/N ratios measured for peaks in C-H or C-C phase spectra by the average S/N ratio measured for the corresponding peaks in the non-phase spectrum. The average value of this ratio (± standard deviation) is reported for each comparison and the number of peaks used to estimate each ratio of S/N ratios is reported in parentheses.

$[3 \times {}^1J(C^\alpha\text{-}H^\alpha)]^{-1}$ (i.e., ~2.6 ms) for non-phase spectra and $2[3 \times {}^1J(C^\alpha\text{-}H^\alpha)]^{-1}$ (~5.2 ms) for phase spectra, assuming ${}^1J(C^\alpha\text{-}H^\alpha) = 128$ Hz. Computer simulations of this transfer function carried out with effective uniform relaxation times $T_{2,eff}$ (defined in the legend of Fig. 2 and assumed to be identical for Gly and non-Gly residues) ranging from 2 to 50 ms indicate that the positions of these optimal τ_{a_f} values are independent of relaxation, although of course the amplitude of the transfer function at these optimal values becomes smaller as the value of $T_{2,eff}$ becomes shorter. In the case of C-C phase tuning (Fig. 2B and 2C), the highest frequency modulation during the $2T_c$ constant-time period for non-Gly spin systems is due to the ${}^1J(C^\alpha\text{-}C^\beta)$ coupling constant. With a uniform relaxation time $T_{2,eff} = 20$ ms, optimal values of $2T_c$ in the HACANH experiment are 6.6 ms (non-phase) and 25.7 ms (phase), respectively, while for the HACA(CO)NH experiments, the corresponding optimum values are 5.7 ms (non-phase) and 26.5 ms (phase), respectively. For both experiments, the positions of these $2T_c$ optima (both phase and non-phase) are relatively independent of relaxation for effective uniform relaxation times $T_{2,eff}$ as small as 15 ms, but shift to smaller values with shorter $T_{2,eff}$ relaxation times.

The coherence transfer functions plotted in Fig. 2 were simulated assuming a uniform relaxation time $T_{2,eff}$ of 20 ms during the entire τ_{a_f} or $2T_c$ periods. This value is based on our experience with uniformly ${}^{15}N,{}^{13}C$-enriched proteins in the 7–14 kDa range. Under these conditions, good signal-to-noise spectra can be obtained using non-phase, C-C phase, or C-H phase delay tunings in proton ($\omega_1 = {}^1H$) and carbon ($\omega_1 = {}^{13}C$) versions of the 3D PFG-CT-HACANH and PFG-CT-HACA(CO)NH experiments. The signal is modulated during the $2T_c$ period by the product of the appropriate $2T_c$ and τ_{a_f} coherence transfer functions. This product is generally smaller for the HACANH experiment than for the HACA(CO)NH experiment. Comparisons of these transfer functions provide a prediction of the best method (C-C or C-H) for obtaining backbone phase information in these two experiments. With this uniform relaxation rate the HACANH experiments yield better S/N ratios using C-C phase methods (i.e. a long $2T_c$ value), while the HACA(CO)NH experiments yield better S/N ratios using C-H phase methods (i.e. a long τ_{a_f} value). Specifically, relative to non-phase spectra ($\tau_{a\_f} = 2.6$ ms, $2T_c = 6.6$ ms) the HACANH experiment should provide better signal-to-noise ratios using C-C Gly phase labeling ($\tau_{a\_f} = 2.6$ ms, $2T_c = 26$ ms) than when using C-H phase labeling ($\tau_{a\_f} = 5.2$ ms, $2T_c = 6.6$ ms). Indeed, in HACANH the signal-to-noise ratios can be better for Gly phase versions than for the non-phase version. This is because longer $2T_c$

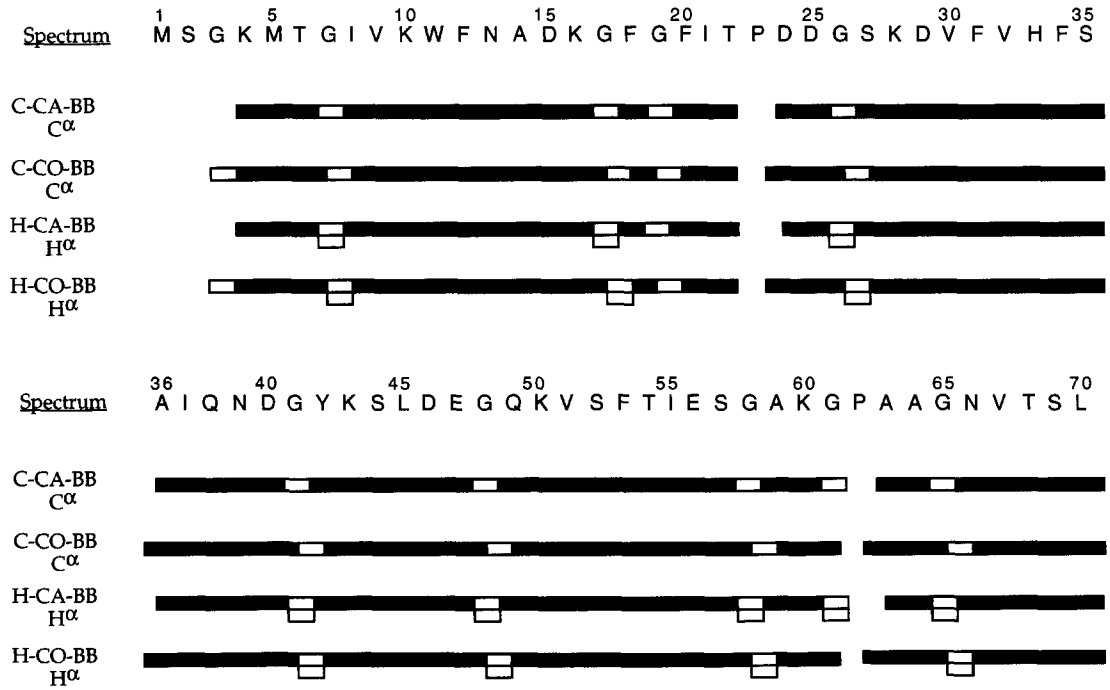

Fig. 4. Sequential connectivity diagram for backbone resonances of CspA obtained from C-C phase PFG-CT-HACANH (designated CA-BB) and C-H phase PFG-CT-HACA(CO)NH (designated CO-BB) 3D triple-resonance experiments described in Fig. 1, using $2T_c$ and τ_{a_f} values described in Table 1. Data were collected with both the $\omega_1 = {}^{13}C$ and $\omega_1 = {}^1H$ versions of these experiments (i.e. C-CA-BB, C-CO-BB, H-CA-BB, and H-CO-BB, respectively). The sample at pH 6.0 and temperature of 30 °C had a protein concentration of ~3 mM. Each 3D time-domain matrix consisted of 64 (t_1, ${}^{13}C$ or ${}^1H$) × 50 (t_2, ${}^{15}N$) × 512 (t_3, H^N) complex data points, and was recorded in a total collection time of about 20 h. Peaks manifesting intraresidue and sequential information in HACANH and HACA(CO)NH data sets are indicated with rectangular bars, which are solid for peaks with positive phase and open for peaks with negative phase.

values used for C-C Gly phase labeling (e.g. $2T_c = 26$ ms) also allow more complete $C^\alpha \rightarrow N$ transfer by the relatively small $^1J(C^\alpha\text{-}N)$ coupling constant (~10 Hz), resulting in better S/N ratios even in the presence of significant C^α relaxation rates. In larger proteins, the effective relaxation rate during the $2T_c$ period is faster, and C-H phase labeling may be preferable. On the other hand, relative to non-phase spectra ($\tau_{a\_f} = 2.4$ ms, $2T_c = 6$ ms) the HACA-(CO)NH experiment is expected to exhibit better signal-to-noise ratios using C-H Gly phase labeling ($\tau_{a\_f} = 4.5$ ms, $2T_c = 9.0$ ms) than with C-C phase labeling ($\tau_{a\_f} = 2.4$ ms, $2T_c = 26$ ms). Since the $^1J(C^\alpha\text{-}C')$ coupling constant is fairly large (~35 Hz), the long $2T_c$ periods required for obtaining C-C phase information cost signal intensity due to relaxation effects and do not enhance the coherence transfer.

These predictions have been verified using a sample of uniformly ^{13}C,^{15}N-enriched cold-shock protein A (CspA) (~7.7 kDa). A representative 2D ^{15}N-^1H correlation spectra obtained using PFG-CT-HACA(CO)NH (Sequence 1A) tuned for C-H-type phase information is shown in Fig. 3. In this projection, the N-H peaks of amides following Gly residues are negative, and the N-H peaks of amides following non-Gly residues are positive. Table 1 presents a comparison of S/N ratios obtained in similar 2D spectra of the HACANH and HACA(CO)NH experiments recorded without phase information (non-phase) and with Gly phase discrimination obtained using either the C-H or C-C methods. As expected from the theoretical plots of Fig. 2, in PFG-CT-HACANH non-Gly spin systems of CspA exhibit better S/N ratios in the C-C phase spectra than in the non-phase spectra. The Gly spin systems themselves exhibit smaller S/N ratios in the C-C phase spectrum compared to the non-phase, which we attribute to shorter carbon transverse relaxation times in methylene compared with methine groups. Although the Gly spin systems for CspA also exhibit slightly better S/N ratios in the C-H phase experiment than in the C-C phase HACANH spectra, in other systems studied the C-C phase HACANH spectra provide slightly better Gly S/N ratios. On the other hand, in PFG-CT-HACA(CO)NH spectra better S/N ratios were obtained for both Gly and non-Gly residues using the C-H phase method.

Figure 4 summarizes the sets of intraresidue and sequential connections obtained for CspA from 3D PFG-CT-HACANH spectra obtained with C-C Gly phase discrimination and 3D PFG-CT-HACA(CO)NH spectra obtained with C-H Gly phase discrimination. Both the $\omega_1 = {}^{13}C$ and $\omega_1 = {}^1H$ versions of the experiments were analyzed. These four 3D data sets were each recorded over approximately 20 h using a protein concentration of ~3 mM. Aside from the N-terminal amide groups which exhibit significant solvent-saturation transfer effects under these conditions and the proline gaps, intraresidue and sequential connections were obtained for the entire sequence with Gly phase discrimination in all four experiments.

The unique chemical shift range of glycine C^α resonances (45.4 ± 1.2 ppm) makes the identification of Gly spin systems relatively easy. However, the experiments described here provide information about both C^α and H^α resonances of glycines. In addition, these experiments provide information about N-H resonances of Gly (or of residues following Gly in the sequence) in the ^{15}N-^1H plane (Fig. 3).

In summary, we have demonstrated optimized proton and carbon versions of PFG-CT-HACANH and PFG-CT-HACA(CO)NH experiments that allow rapid and almost complete assignments of backbone H^α, $^{13}C^\alpha$, ^{15}N and H^N resonances in small (< 20 kDa) proteins. These four experiments form part of a series of several experiments currently used in our laboratory as input for automated computer analysis of resonance assignments (Zimmerman et al., 1996). This work provides a practical guide to using these experiments for determining resonance assignments in proteins and for identifying both intraresidue and sequential connections involving glycine residues. Two types of delay tuning provide phase discrimination of backbone Gly C^α and H^α resonances: (i) C-H phase tuning of the refocusing period τ_{a_f}; and (ii) C-C phase tuning of the ^{13}C constant-time evolution period $2T_c$. For small proteins, C-C phase tuning provides better S/N ratios in PFG-CT-HACANH experiments while C-H phase tuning provides better S/N ratios in PFG-CT-HACA(CO)NH. 'Straight-through'-type experiments like those described here are especially amenable to this kind of phase tuning for aliphatic spin-system topologies, though similar experiments could be designed using 'out-and-back'-type magnetization-transfer pathways (Gehring and Guittet, 1995). These same principles can also be applied in triple-resonance experiments utilizing ^{13}C-^{13}C COSY and TOCSY to correlate peripheral side-chain atoms and backbone amide protons for classifying side-chain spin-system topologies (Grzesiek and Bax, 1993; Tashiro et al., 1995; Rios et al., 1996). Similar phase-tuning methods should find many other applications for spectral editing in triple-resonance experiments. Efforts to incorporate such 'phase data' into algorithms for automated analysis of resonance assignments in proteins (Zimmerman and Montelione, 1995) are in progress in our laboratory.

Acknowledgements

We thank Z. Shang, G.V.T. Swapna and M. Tashiro for helpful discussions and comments on the manuscript. This work was supported by grants from Pharmacia-Upjohn Inc., the National Institutes of Health (GM-47014), the National Science Foundation (MCB-9407569), a National Science Foundation Young Investigator Award (MCB-9357526 to G.T.M.), and a Camille Dreyfus Teacher-Scholar Award (to G.T.M.).

References

Bax, A. and Grzesiek, S. (1993) *Acc. Chem. Res.*, **26**, 131–138.

Boucher, W., Laue, E.D., Campbell-Burk, S.L. and Domaille, P.J. (1992) *J. Biomol. NMR*, **2**, 631–637.

Clubb, R.T., Thanabal, V. and Wagner, G. (1992) *J. Magn. Reson.*, **97**, 213–217.

Friedrichs, M., Mueller, L. and Wittekind, M. (1994) *J. Biomol. NMR*, **4**, 703–726.

Gehring, K. and Guittet, E. (1995) *J. Magn. Reson.*, **B109**, 206–208.

Grzesiek, S. and Bax, A. (1992a) *J. Am. Chem. Soc.*, **114**, 6291–6293.

Grzesiek, S. and Bax, A. (1992b) *J. Magn. Reson.*, **99**, 201–207.

Grzesiek, S. and Bax, A. (1993) *J. Biomol. NMR*, **3**, 185–204.

Grzesiek, S. and Bax, A. (1995) *J. Am. Chem. Soc.*, **117**, 6527–6531.

Ikura, M., Kay, L.E. and Bax, A. (1990) *Biochemistry*, **29**, 4659–4667.

Kay, L.E., Ikura, M. and Bax, A. (1991) *J. Magn. Reson.*, **91**, 84–92.

Kay, L.E., Wittekind, M., McCoy, M.A., Friedrichs, M.S. and Mueller, L. (1992a) *J. Magn. Reson.*, **98**, 443–450.

Kay, L.E., Keifer, P. and Saarinen, T. (1992b) *J. Am. Chem. Soc.*, **114**, 10663–10665.

Lyons, B.A. and Montelione, G.T. (1993) *J. Magn. Reson.*, **101**, 206–209.

Marion, D., Ikura, M., Tschudin, R., and Bax, A. (1989) *J. Magn. Reson.*, **84**, 393–399.

Meadows, R.P., Olejniczak, E.T. and Fesik, S.W. (1994) *J. Biomol. NMR*, **4**, 79–96.

Morris, G. (1980) *J. Am. Chem. Soc.*, **102**, 428–429.

Montelione, G.T. and Wagner, G. (1989a) *J. Am. Chem. Soc.*, **111**, 3096–3098.

Montelione, G.T. and Wagner, G. (1989b) *J. Am. Chem. Soc.*, **111**, 5474–5475.

Montelione, G.T. and Wagner, G. (1990) *J. Magn. Reson.*, **83**, 183–188.

Montelione, G.T., Lyons, B.A., Emerson, S.D. and Tashiro, M. (1992) *J. Am. Chem. Soc.*, **114**, 10974–10975.

Nagayama, K. (1986) *J. Magn. Reson.*, **66**, 240–249.

Olejniczak, E.T., Xu, R.X., Petros, A.M. and Fesik, S.W. (1992) *J. Magn. Reson.*, **100**, 444–450.

Olejniczak, E.T. and Fesik, S.W. (1994) *J. Am. Chem. Soc.*, **116**, 2215–2216.

Palmer, A.G., Fairbrother, W.J., Cavanagh, J., Wright, P.E. and Rance, M. (1992) *J. Biomol. NMR*, **2**, 103–108.

Powers, R., Gronenborn, A.M., Clore, G.M. and Bax, A. (1991) *J. Magn. Reson.*, **94**, 209–213.

Rios, C.B., Feng, W., Tashiro, M., Shang, Z. and Montelione, G.T. (1996) submitted to *J. Biomol. NMR*.

Santoro, J. and King, G.C. (1992) *J. Magn. Reson.*, **97**, 202.

Shaka, A.J., Barker, P.B. and Freeman, R. (1985) *J. Magn. Reson.*, **64**, 547–552.

Tashiro, M., Rios, C.B. and Montelione, G.T. (1995) *J. Biomol. NMR*, **6**, 211–216.

Wittekind, M. and Mueller, L. (1993) *J. Magn. Reson.*, **B101**, 201–205.

Wittekind, M., Metzler, W.J. and Mueller, L. (1993) *J. Magn. Reson.*, **B101**, 214–217.

Yamazaki, T., Forman-Kay, J.D. and Kay, L.E. (1993) *J. Am. Chem. Soc.*, **115**, 11054–11055.

Yamazaki, T., Pascal, S.M., Singer, A.U., Forman-Kay, J.D. and Kay, L.E. (1995) *J. Am. Chem. Soc.*, **117**, 3556–3564.

Zimmerman, D.E. and Montelione, G.T. (1995) *Curr. Opin. Struct. Biol.*, **5**, 664–673.

Zimmerman, D., Kulikowski, C., Wang, L., Lyons, B. and Montelione, G.T. (1994) *J. Biomol. NMR*, **4**, 241–256.

Zimmerman, D.E., Kulikowski, C.A., Feng, W., Tashiro, M., Chien, C.-Y., Rios, C.B., Moy, F.J., Powers, R. and Montelione, G.T. (1996) manuscript submitted for publication.